Journal of Modern Optics
Vol. 00, No. 00, DD Month 200x, 1–19

Speed-up and slow-down collisions in laser-induced nonsequential multiple ionization

C. Figueira de Morisson Faria*[1] and X. Liu[2]
[1]Centre for Mathematical Science, City University, Northampton Square, London EC1V OHB, UK
[2]Department of Physics, Texas A&M University, College Station, TX 77843-4242, USA

(Received 00 Month 200x; In final form 00 Month 200x)

We investigate laser induced nonsequential multiple ionization using a simple statistical model in which an electron recollides inelastically with its parent ion. In this collision, it thermalizes with the remaining $N-1$ bound electrons within a time interval Δt. Subsequently, all the N electrons leave. We address the question of how the above time delays influence the individual contributions from the orbits in which the first electron, upon return, is accelerated or decelerated by the field, respectively, to the ion momentum distributions. In both cases, the time delays modify the drift momenta obtained by the N electrons when they reach the continuum at $t+\Delta t$, by moving such times towards or away from a crossing of the electric field. The contributions from both types of collisions are influenced in distinct ways, and the interplay between such trends determines the widths and the peak momenta of the distributions. Specifically in the few-cycle pulse case, we also show that such time delays do not affect the shapes of the momentum distributions in a radical fashion. Hence, even with a thermalization time Δt, nonsequential multiple ionization could in principle be used for absolute-phase diagnosis.

1 Introduction

The physics of non-sequential double ionization in rare gases by low-frequency, intense laser fields is, to a very large extent, understood. In particular for neon, the electron momentum distributions with peaks at non-vanishing momentum components $p_{1||}=p_{2||}=\pm 2\sqrt{U_p}$, along the laser-field polarization, or the ion momentum distributions peaked at the parallel momenta $P_{||}=\pm 4\sqrt{U_p}$, where U_p denotes the ponderomotive energy, can be explained by a laser-induced inelastic recollision process [1–3]. Specifically, the first electron leaves an atom by tunneling ionization at a time t', propagates in the continuum, being accelerated by the field and, subsequently, at a time t, recollides with its parent ion. The second electron is then freed by electron-impact ionization [4].

*Corresponding author. E-mail: c.f.m.faria@city.ac.uk

This process has been successfully dealt with using an S-Matrix approach and its classical counterpart [5–9]. In particular, if the laser-field intensity is high enough, both quantum-mechanical and classical models yield very similar momentum distributions[1]. We have shown that this agreement occurs for several types of electron-electron interaction, and in the absence or presence of Coulomb repulsion in the electron final states [6–8]. Furthermore, we have verified that the outcome of the classical and quantum mechanical computations also exhibit a striking agreement if the driving field is a few-cycle laser pulse [9, 12]. In particular, both the classical and quantum mechanical distributions are strongly dependent on the so-called absolute phase, i.e., the phase difference between the pulse envelope and its carrier oscillation. We have used this fact in order to propose a scheme for diagnosing the absolute phase [12], which has also been experimentally realized [13].

If one is dealing, however, with more than two active electrons, there are many open questions concerning the physics behind laser-induced multiple ionization. This is in particular true for triple and quadruple ionization of neon by near infra-red ($\omega = 0.057$ a.u.) laser fields in an intensity range below 2×10^{15} W/cm^2 [2, 14, 15]. The distributions observed in such experiments, approximately peaked at non-vanishing ion momenta $P_{||} = \pm 2N\sqrt{U_p}$, where N denotes the number of electrons involved, hint at a non-sequential physical mechanism. The theoretical modeling of non-sequential multi-electron processes for $N > 2$, however, poses a far greater challenge than in the two-electron case. For instance, already for three electrons, which is the simplest scenario to be taken into consideration, one must include at least six Feynman diagrams when computing the corresponding transition amplitude, each of which is rather cumbersome to implement.

In order to tackle such a problem, in previous work [16], we constructed a simple thermalization model, similar to those employed in, for instance, nuclear [17] or molecular [18] physics. We assumed that the first electron, upon return, recollides with its parent ion and shares its kinetic energy with $N-1$ bound electrons. All the N electrons are then freed after a time interval Δt subsequent to the recollision time t, which, to first approximation, is taken to be constant. We regard this time as the upper bound for a thermalization time, which is necessary for the kinetic energy to be redistributed among the N electrons.

The above-mentioned process takes place within a fraction of the cycle of the laser field. Since the duration of a typical titanium-sapphire pulse, employed in such experiments, is of the order of 2.7 fs, Δt falls within the attosecond

[1]This, however, no longer holds if the intensity is near threshold, i.e., just enough for the second electron to be released. For a detailed discussion c.f. [10], and for measurements of nonsequential double ionization below the threshold see, e.g., [11].

regime. Indeed, recently, by comparing our thermalization model with the available experimental data for triple and fourfold ionization of neon [14,15], we have been able to estimate thermalization times of the order of 460 attoseconds [16]. Using such a time delay, we computed ion momentum distributions whose widths and peak momenta agreed very well with those in the experiments.

To a very large extent, our thermalization model contains classical ingredients and is a generalization of the classical model already employed in the two-electron case [7, 8]. In [16], we have also observed that the peaks and the width of the momentum distributions depend very strongly on the time delay Δt. The position of the peaks is a direct consequence of the kinematics involved in the process, as the final drift momentum the N electrons acquire from the field, will strongly depend on the time $t + \Delta t$ when they reach the continuum.

The above-stated physical mechanism, however, is not completely agreed upon. Indeed, it could well be that a broadening in the electron momentum distributions and the displacement in the peak momenta are caused by, for instance, partially sequential ionization processes [15], or excitation tunneling mechanisms [19] , in which, during the recollision, the electrons undergo a transition to an excited state, from which they subsequently tunnel (for an example of such mechanisms for different atomic species see, e.g., [20]). Specifically for large thermalization times, the distributions are very much concentrated near vanishing parallel momenta, and resemble those obtained with excitation-tunneling. Apart from that, even assuming that thermalization through electron-impact ionization is the only or at least the dominant physical mechanism, it is not clear how the time delay Δt affects the width of the distributions.

Another open question concerns the influence of the types of collisions on the momentum distributions. In fact, for the recombination or rescattering phenomena occurring in the context of atoms in strong laser fields, there exist two main orbits along which an electron may return to its parent ion with the same kinetic energy. Such orbits are known as "the long orbit", or "the short orbit", and have been extensively investigated in the context of high-order harmonic generation and above-threshold ionization [21] and, more recently, for nonsequential double ionization [22, 23]. An electron following the long orbit leaves the atom at a time $t' < 0.3T$, where $T = 2\pi/\omega$ denotes a field cycle, and returns after the minimum of the electric field, whereas an electron along the short orbit reaches the continuum at $t' > 0.3T$ and returns before the minimum of the electric field. Hence, in the former and in the latter case the returning electron is decelerated and accelerated by the field, respectively.

In recent years, both orbits have been investigated in the context of nonsequential double ionization using classical ensemble models [22]. In particular, they have been associated to two main types of collisions. The orbits for which

the electron is being decelerated have been related to the so-called "slow-down collisions", whereas the short orbit has been linked to the so-called "speed-up collisions". Depending on several parameters, such as the field intensity or frequency, one type of collisions may provide the dominant contributions to the yield, or both types may be equally important [27]. For instance, for the parameters in [22], it was shown that the slow-down collisions dominate.

In this paper, we address the question of how the contributions from the short and the long orbit to the multiple-ionization momentum distributions are affected by the time delay Δt, for triple and fourfold ionization. We are mainly concerned with the influence of both sets of orbits on the width and the peaks of the ion momentum distributions, for resolved and non-resolved ion momentum components transverse to the laser-field polarization. We take the driving field to be a monochromatic wave or a few-cycle pulse, and make a detailed analysis of the similarities and differences between both cases. This manuscript is organized as follows: In the subsequent section, we provide a brief discussion of our thermalization model, with the explicit expressions for the ion momentum distributions. In Sec. 3, we display our results for the different sets of orbits, together with the total yields and, finally, in Sec. 4, we state our conclusions.

2 Model

We will briefly recall the statistical model employed in our previous publication [16], in order to determine the momentum distributions in N-fold nonsequential ionization. This model is mainly composed by three main ingredients.

Firstly, we assume that one electron tunnels into the continuum at an instant t' according to the quasi-static rate [25].

$$R(t') \sim |E(t')|^{-1} \exp\left[-2(2|E_{01}|)^{3/2}/(3|E(t')|)\right], \tag{1}$$

where $E(t')$ and $|E_{01}|$ denote the electric field at the time the electron left and the first ionization potential, respectively.

Subsequently, this electron propagates under the sole influence of the laser field, and obeys the classical equations of motion. At a later time t, it may be driven back towards its parent ion, recolliding inelastically with it. The return condition $\mathbf{r_1}(t) = 0$ for the first electron yields

$$F(t) = F(t') + (t - t')A(t'), \tag{2}$$

where $\mathbf{A}(t)$ is the vector potential, and $F(t) = \int^t A(\tau)d\tau$. Eq. (2) provides a

clear geometrical picture for the return condition: for a given t', the return time t is given by the intersection of $F(t)$ with its tangent at t' [26]. We will employ this construction in Sec. 3, when discussing our results (c.f. Fig. 2).

Upon recollision, the energy $E_{\rm ret}(t) = [A(t) - A(t')]^2/2$ of the returning electron is completely thermalized among such an electron *and* the $N-1$ electrons to be freed. After the time interval Δt, the distribution of energy and momentum over the N electrons is only governed by the available phase space. We will consider here that the time delay Δt is constant. Finally, at the time $t+\Delta t$, the N electrons reach the continuum with the total kinetic energy $E_{\rm ret} - E_0^{(N)}$. The quantity $E_0^{(N)} = \sum_{n=2}^{N} |E_{0n}|$ denotes the total ionization potential of the $N-1$ (up to the recollision time t inactive) electrons.

The distribution of final electron momenta $\mathbf{p}_n$ $(n = 1, \ldots, N)$ is proportional to

$$F(\mathbf{p}_1, \mathbf{p}_2, \ldots, \mathbf{p}_N) = \int dt' R(t') \delta \left(E_0^{(N)} - E_{\rm ret}(t) + \frac{1}{2} \sum_{n=1}^{N} [\mathbf{p}_n + \mathbf{A}(t+\Delta t)]^2 \right), \tag{3}$$

where $\mathbf{p}_n$, and $\mathbf{A}(t+\Delta t)$ denote the final electron momenta and the vector potential at the time the electron leaves, respectively. The integral extends over the ionization time t'. The δ function expresses the fact that the total kinetic energy of the N participating electrons is fixed by the first-ionized electron at its recollision time t.

In the $3-N$ dimensional momentum space $(\mathbf{p}_1, \ldots, \mathbf{p}_N)$, the argument of the δ function corresponds to the equation of a hypersphere

$$\frac{1}{2} \sum_{n=1}^{N} [p_{n\parallel} + A(t+\Delta t)]^2 + \frac{1}{2} \sum_{n=1}^{N} \mathbf{p}_{n\perp}^2 = E_{\rm ret}(t) - E_0^{(N)}, \tag{4}$$

where $p_{n\parallel}$ and $\mathbf{p}_{n\perp} (n = 1, ..., N)$ denote the electron momentum components parallel and perpendicular to the laser-field polarization, centered at $-A(t+\Delta t)$, and whose radius is determined by the difference between the kinetic energy $E_{\rm ret}(t)$ of the first electron upon return and the absolute value $E_0^{(N)}$ of the total binding energy which must be overcome. Within the region delimited by this hypersphere, in a classical framework, the process we are dealing with takes place. Furthermore, if the transverse momenta are kept constant, Eq.

(4) can be written as

$$\frac{1}{2}\sum_{n=1}^{N}[p_{n\parallel}+A(t+\Delta t)]^2 = E_{\rm ret}(t) - \tilde{E}_0^{(N)}, \tag{5}$$

where $\tilde{E}_0^{(N)} = E_0^{(N)} + \frac{1}{2}\sum_{n=1}^{N}\mathbf{p}_{n\perp}^2$ can be regarded as an effective binding energy which the N electrons must overcome. Such an energy depends on the transverse momentum components, and is minimal when they vanish. By employing an adequate choice of field and atomic parameters, such as, for instance, a few-cycle pulse, one can manipulate the radius in (4), making whole momentum regions collapse or appear. In [9,12], we have exploited this in the two-electron case in order to determine the absolute phase.

The only free parameter of this model is the time delay Δt between the recollision time and the time when multiple ionization occurs. It is the sum of the time it takes to establish the statistical ensemble, i.e., the thermalization time, and a possible additional "dwell time", until the electrons become free. This model is an extension to NSMI of a classical model introduced for NSDI in Refs. [7,8] for $\Delta t = 0$. Sufficiently high above threshold, it produced momentum distributions that were virtually indistinguishable from their quantum-mechanical counterparts.

In order to integrate over unobserved momentum components, we exponentialize the δ function in Eq. (3) using its Fourier representation

$$\delta(x) = \int_{-\infty}^{\infty}\frac{d\lambda}{2\pi}\exp(-i\lambda x). \tag{6}$$

Infinite integrations over the momenta $\mathbf{p}_n$ can then be done by Gaussian quadrature. The remaining integration over the variable λ is performed employing [28]

$$\int_{-\infty}^{\infty}\frac{d\lambda}{(i\lambda+\epsilon)^\nu}e^{ip\lambda} = \frac{2\pi}{\Gamma(\nu)}p_+^{\nu-1}, \tag{7}$$

where $x_+^\nu = x^\nu\theta(x)$, with $\theta(x)$ the unit step function and $\epsilon \to +0$.

The momentum distribution of the ion is then

$$\begin{aligned} F(\mathbf{P}) &\equiv \int\prod_{n=1}^{N}d^3\mathbf{p}_n\delta\left(\mathbf{P}+\sum_{n=1}^{N}\mathbf{p}_n\right)F(\mathbf{p}_1,\mathbf{p}_2,\ldots,\mathbf{p}_N) \\ &= \frac{(2\pi)^{\frac{3N}{2}-\frac{3}{2}}}{N^{3/2}\Gamma(3(N-1)/2)}\int dt' R(t')\left(\Delta E_{N,\rm ion}\right)_+^{\frac{3N}{2}-\frac{5}{2}} \end{aligned} \tag{8}$$

with $\Delta E_{N,\mathrm{ion}} \equiv E_{\mathrm{ret}}(t) - E_0^{(N)} - \frac{1}{2N}[\mathbf{P} - N\mathbf{A}(t+\Delta t)]^2$, where $\mathbf{P}$ gives the momentum of the ion. In (8), we have used the momentum conservation $\mathbf{P} = -\sum_{n=1}^{N} \mathbf{p}_n$, which is valid in case the photon momenta can be neglected.

If the ion momentum component perpendicular to the laser polarization is entirely integrated over, the remaining distribution of the longitudinal ion momentum $P_\parallel$ reads

$$\begin{aligned} F(P_\parallel) &\equiv \int d^2\mathbf{P}_\perp F(\mathbf{P}) \\ &= \frac{(2\pi)^{\frac{3N}{2}-\frac{1}{2}}}{\sqrt{N}\Gamma((3N-1)/2)} \int dt' R(t') \left(\Delta E_{N,\mathrm{ion}\parallel}\right)_+^{\frac{3N}{2}-\frac{3}{2}}, \end{aligned} \tag{9}$$

where $\Delta E_{N,\mathrm{ion}\parallel} \equiv E_{\mathrm{ret}}(t) - E_0^{(N)} - \frac{1}{2N}[P_\parallel - NA(t+\Delta t)]^2$.

If just one transverse-momentum component (for instance, $P_{\perp,2}$) is integrated while the other one ($P_{\perp,1} \equiv P_\perp$) is observed, the corresponding distribution is

$$\begin{aligned} F(P_\parallel, P_\perp) &\equiv \int dP_{\perp,2} F(\mathbf{P}) \\ &= \frac{(2\pi)^{\frac{3N}{2}-1}}{N\Gamma(3N/2-1)} \int dt' R(t') \left(\Delta E_{N,\mathrm{ion}\parallel\perp}\right)_+^{\frac{3N}{2}-2} \end{aligned} \tag{10}$$

with $\Delta E_{N,\mathrm{ion}\parallel\perp} \equiv \Delta E_{\mathrm{ion}\parallel} - \frac{1}{2N}P_\perp^2$. In the following section we will explicitly compute ion momentum distributions employing our thermalization model, i.e., from Eqs. (9) and (10).

3 Momentum distributions

3.1 *Monochromatic fields*

As a starting point, we will consider a monochromatic laser field $\mathbf{E}(t) = -d\mathbf{A}(t)/dt$, for which the vector potential is of the form

$$\mathbf{A}(t) = A_0 \cos(\omega t)\hat{e}_z, \tag{11}$$

with frequency ω, amplitude A_0 and polarization axis $\hat{e}_z$. This is a good approximation for long pulses. In this case, $\Delta E_{N,\mathrm{ion}\parallel}(P_{||}, t) = \Delta E_{N,\mathrm{ion}\parallel}(-P_{||}, t + T/2)$, where $T = 2\pi/\omega$ denotes a period of the driving field, so that the momentum distributions are symmetric with respect to $P_{||} = 0$. Clearly, this also

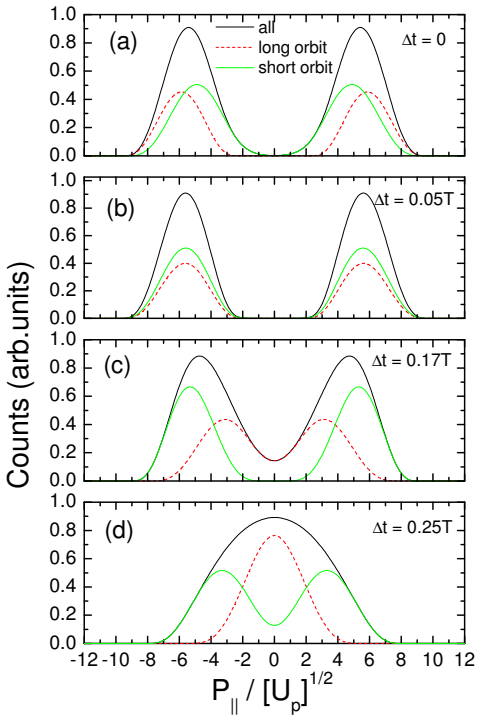

Figure 1. (Color online) Distribution of the longitudinal ion momentum for triple nonsequential ionization of neon at $I = 2 \times 10^{15}\mathrm{W/cm}^2$, for time delays $\Delta t = 0$, $\Delta t = 0.05T$, $\Delta t = 0.17T$, and $\Delta t = 0.25T$, together with individual contributions from the long and the short orbits. The ion momenta are given in units of $[Up]^{1/2}$

holds for $\Delta E_{N,\mathrm{ion}\|\perp}$. In our computations, we consider the shortest pair of trajectories along which the first electron returns to its parent ion, and, in particular, the individual contributions from the longer and the shorter orbit within such a pair. Such orbits coalesce at the boundary of the region determined by the hypershpere (4) for which, classically, nonsequential multiple ionization is allowed to occur. In the particular model employed in this paper, such a boundary is determined by the minimal momenta the N electrons need in order to overcome the binding energy $E_0^{(N)}$, and the maximal momenta for which the first electron is able to return.

In Fig. 1, we display the yield computed assuming that the first electron returns to its parent ion either along the long or the short orbit, together with the total momentum distributions, for triple ionization of neon. In the upper panel [Fig. 1.(a)], the thermalization time is taken to be vanishing. As an overall feature, the total yield is approximately peaked at $P_{||} = \pm 6\sqrt{U_p}$, as expected from classical arguments. Furthermore, the shorter orbit yields

distributions which are slightly shifted towards lower momenta, in comparison to those from the longer orbit. Such a shift is corrected if a time delay $\Delta t = 0.05T$ is introduced [Fig. 1.(b)]. This can be easily understood in terms of the momentum transfer from the field to the electrons. Such a momentum transfer is maximal if all electrons leave at a crossing of the field, i.e., for $t + \Delta t = n\pi$. For vanishing time delay, the electrons released by a speed up collision, i.e., by an electron returning along the short orbit, leave at roughly $t_S = 0.95T$, while for the slow-down collisions, this happens at $t_L = 1.05T$. The time delay $\Delta t = 0.05T$ moves the release times $t_s + \Delta t$ for the short-orbit contributions towards the crossing and their long-orbit counterparts $t_s + \Delta t$ away from it. As a direct consequence, the contributions from the former set of orbits move towards higher absolute momenta, while those from the latter set move towards lower absolute momenta.

If the time delay increases [Fig. 1.(c)], the peak momenta from the short-orbit contributions starts to move again towards lower absolute values. This is due to the fact that, for $\Delta t > 0.05T$, the time $t_S + \Delta t$ all electrons leave starts to move away from the crossing of the driving field. Hence, the drift momenta of the electrons freed by the speed-up collisions decrease. One should note, however, that the times $t_L + \Delta t$, for the electrons released by the slow-down collisions, also move farther away from the crossing. In this latter case, however, the peak momenta decrease in a far more radical way. The fact that the two individual contributions are now peaked at momenta which are very far apart leads to a broadening in the momentum distributions. In this context, it is worth mentioning that the time delay $\Delta t = 0.17T$ yields the best agreement with the experimental findings, for nonsequential triple and quadruple ionization [14, 15]. This issue is discussed in more detail in [16].

For exceptionally large time delays, such as those depicted in Fig. 1.(d), the contributions from the short orbit move back to lower momenta, and those from the long orbit overlap at vanishing ion momenta. As a direct consequence, the total yield merges in a single peak at vanishing momentum. Such features resemble to a very large extent those obtained if one considers sequential physical mechanisms, or the situation where the electrons undergo a transition to an excited state, and, subsequently, tunnel into the continuum. One should note, however, that for such a parameter range, there is poor agreement with the experimental results.

The effect observed in Fig. 1 is shown in more detail in Fig. 2, using the tangent construction mentioned in the previous section. In the figure, we consider the return condition (2) for the short and long orbits. For vanishing time delays, the electron starting at t'_S and t'_L releases the remaining electrons at the times t_S before or t_L after the crossing of the field, respectively. Such times are determined by the intersection of the tangents (2) with the dashed line. If, however, there is a time delay Δt, the time $t + \Delta t$ in which all electrons leave

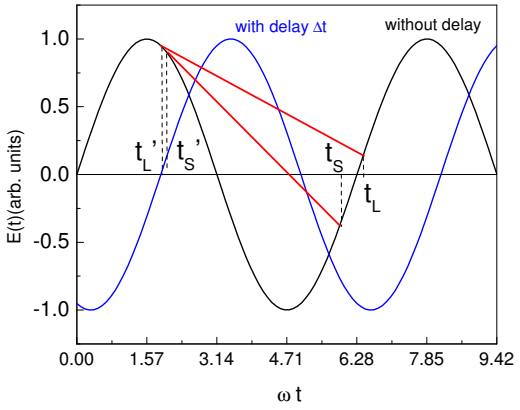

Figure 2. (Color online) Start and return times for the long and short orbits, denoted by (t'_L, t_L), (t'_S, t_S), respectively, for vanishing and non-vanishing time delays Δt.

will be determined by the intersection of the tangents (2) with the *solid* line.

In Fig. 3, we depict the contributions from the slow-down and the speed-up collisions, as well as from the total yield, for the quadruple-ionization case and the same time delays as in Fig. 1. They exhibit the same overall behavior as in Fig. 1: the peak momenta for the short-orbit contributions moves towards higher absolute values for $\Delta t = 0.05T$ [Fig. 3.(b)], and, as Δt is further increased, the peak momenta start to decrease [Fig. 3.(c)]. The maxima of the long-orbit contributions always shift towards $P_{||} = 0$, for increasing Δt, as shown in Fig. 3.(b)-(d). This behavior is expected, since within our model, both triple and quadruple nonsequential ionization are governed by the same physical mechanism, namely energy transfer to all active electrons due to the recollision of the first electron with its parent ion. The main difference is the fact that all electrons must overcome a larger energy $E_0^{(4)}$ in order to reach the continuum. Therefore, for the same laser-field intensity, as the charge state increases, the radius of the hypersphere (4) decreases and so does the momentum region for which the process in question occurs. Furthermore, the peak momenta should increase to the vicinity of $P_{||} = \pm 8\sqrt{U_p}$. This leads, in general, to distributions which are much more localized around the maxima than in the triple-ionization case.

For a time delay $\Delta t = 0.25T$, however, instead of a single peak at vanishing momenta, the total distribution exhibits a plateau, with humps near its low- and high-energy ends [Fig. 3 .(d)] . This is due to the fact that, while the region near $P_{||} = 0$ is filled by the contributions from the long orbit, the contributions from the short orbit are still at a much larger momenta than in the two electron

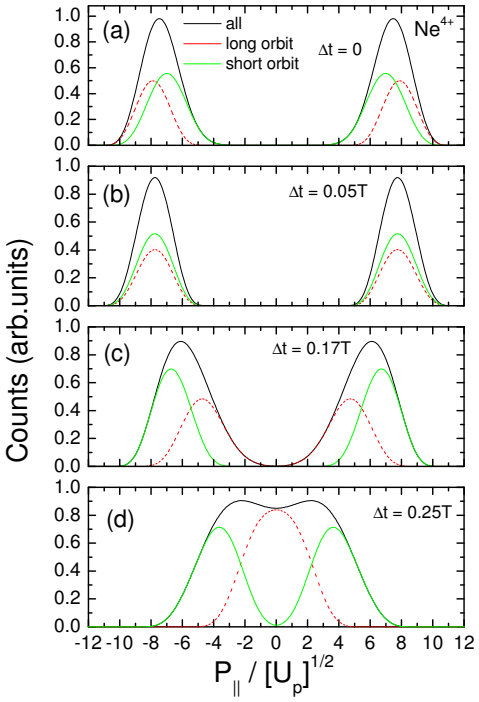

Figure 3. (Color online) Distribution of the longitudinal ion momentum for quadruple nonsequential ionization of neon at $I = 2 \times 10^{15}\mathrm{W/cm^2}$, for time delays $\Delta t = 0$, $\Delta t = 0.05T$, $\Delta t = 0.17T$, and $\Delta t = 0.25T$, together with individual contributions from the long and the short orbits. The ion momenta are given in units of $[U_p]^{1/2}$.

case, and still cause such humps. However, the distributions from the negative and positive momentum regions still merge, as in the triple-ionization case.

Finally, in Fig. 4, we analyze the individual contributions of both orbits if the transverse momenta are only partly integrated over, for time delays $\Delta t = 0$ and $\Delta t = 0.17T$. The distributions from the short and the long orbits exhibit a displacement in their peak momenta which is similar to those obtained in the non-resolved case. In particular, the elongation observed in experiments for such distributions is directly related to this displacement.

3.2 *Few-cycle pulses*

In this section, we will take the driving field to be a few-cycle pulse $\mathbf{E}(t) = -d\mathbf{A}(t)/dt$, corresponding to the vector potential

$$\mathbf{A}(t) = A_0 \sin^2[\omega t/(2n)] \sin(\omega t + \phi)\hat{e}_z \tag{12}$$

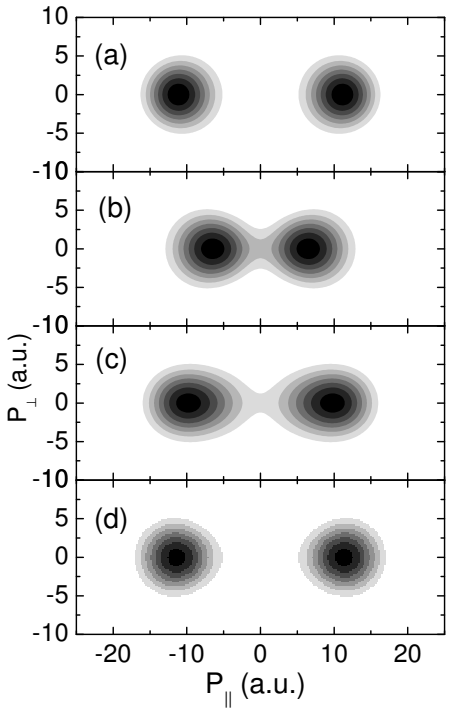

Figure 4. Ion momentum distribution of nonsequential triple ionization of neon at $I = 1.5 \times 10^{15}\mathrm{W/cm^2}$, and time delay $\Delta t = 0.17T$. Panels (a), (b) and (c) correspond to the contributions of the short orbit, of the long orbit, and to the total yield, respectively. In panel (d), the total yield for vanishing time delay is given for comparison. The ion momenta are given in atomic units.

where ϕ is the absolute phase, and n is the number of cycles. We choose a four-cycle pulse ($n = 4$), and consider triple and quadruple ionization. Apart from their wide range of applications (for reviews see, e.g., [24]), few-cycle pulses are very attractive in the context of nonsequential multiple ionization. This is due to the fact that several physical mechanisms which would compete with electron-impact ionization, such as excitation-tunneling ionization, are strongly suppressed in the few-cycle case [14]. Therefore, in principle, one expects cleaner measurements.

In Fig. 5, we present ion momentum distributions for triple ionization of neon, computed with the driving field (12). As a starting point, we take the thermalization time Δt to be vanishing. In contrast to the monochromatic case, such distributions are in general asymmetric with respect to $P_{\|} = 0$. This is expected since, for a few cycle pulse, $A(t) = \pm A(t + nT/2)$ holds, if at all, only for very specific sets of parameters. Therefore the relation $\Delta E_{N,\mathrm{ion}\|}(P_{||}, t) = \Delta E_{N,\mathrm{ion}\|}(-P_{||}, t + T/2)$ is in general not fulfilled. Depend-

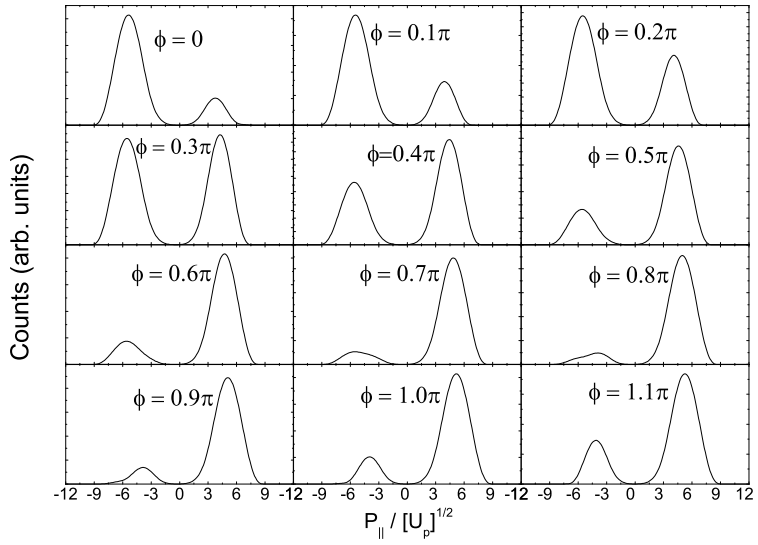

Figure 5. Ion momentum distribution of nonsequential triple ionization of neon by a four cycle pulse of intensity $I = 2 \times 10^{15}\mathrm{W/cm}^2$, and several absolute phases ϕ. We assume that the electrons leave instantaneously after recollision ($\Delta t = 0$). The ion momenta are given in units of $[U_p]^{1/2}$.

ing on the absolute phase, the distributions are strongly localized in either the positive or negative momentum region. Around a critical phase, they start to shift from one momentum region to the other.

Such a behavior is very similar to that observed for nonsequential double ionization ($N = 2$). In the two-electron case, this shift has been employed to diagnose the absolute phase [9, 12, 13]. Furthermore, it has been explained as a change in the dominant set of trajectories for an electron rescattering with its parent ion. Such a set is determined by the interplay between the rate (1) with which the first electron is released in the continuum, and the available phase space: if there was a large probability for the first electron to leave along a particular set of orbits, and if it returned with enough energy to cause appreciable electron-impact ionization, one expects the contributions from such orbits to the yield to be large.

Within the present model, this explanation also holds for $N > 2$, and is illustrated in Fig. 6 for the parameter set of Fig. 5. In the upper and lower panels, we present the quasi-static tunneling rate and parallel momentum components for the residual ion, respectively, as functions of the emission time t'. In the latter case, we consider the transverse ionic momentum components to be vanishing. This gives an upper bound for the momentum region for which electron-impact ionization is allowed to occur, since, in Eq. (5), the effective

binding energy $\tilde{E}_0^{(N)}$ is minimal.

In the figure, we identify at least three sets of orbits, whose start times t' are highly dependent on the carrier-envelope phase ϕ. For instance, for $\phi = 0$, there exist three such pairs: $(1,2)$, $(3,4)$ and $(5,6)$. Thereby, the odd and even numbers refer to the longer and the shorter orbit in a pair, respectively. Orbits $(1,2)$ and $(5,6)$ contribute to the yield in the positive momentum region, whereas $(3,4)$ leads to a peak in the region $P_\parallel < 0$. Since, for $(1,2)$, the quasi-static rate (1) is very small, the contributions from this set of orbits is negligible. Hence, the features observed in Fig. 5 will be determined by the remaining two pairs. In fact, orbits $(3,4)$ and $(5,6)$ lead to the large peak for negative momenta and to the small peak for positive momenta, respectively. For the set $(3,4)$, there is a large momentum region for which the first electron may dislodge the remaining two, and a non-negligible ionization rate. Therefore, its contributions to the yield are expected to be quite prominent. For the set $(5,6)$, even though the tunneling rate is very large, there is only a small region for which electron-impact ionization is allowed. Hence, the pair $(3,4)$ dominates.

This picture starts to change around the critical phase $\phi_c = 0.3\pi$, for which the yield is approximately symmetric. In comparison to the case $\phi = 0$, there is now a decrease in the quasi-static rate for $(3,4)$ and an increase in the momentum region for $(5,6)$. Therefore, the contributions from the former orbits decrease and those from the latter orbits increase, respectively. Beyond the critical phase (for instance, for $\phi = 0.8\pi$), the yield is mainly concentrated in the positive momentum region, since now $(5,6)$ prevail. For this latter case, there is also a further set of orbits which contribute to the yield in the region $P_\parallel < 0$, namely $(7,8)$. For such a set, the rate (1) is very large. However, the region for which electron-impact ionization is allowed to occur is very small and $(5,6)$ is still the dominant pair of orbits.

For a higher charge state, the very same line of argumentation applies. The main difference is that the first electron will need to overcome a larger binding energy in order to release the remaining electrons. As a direct consequence, the radius of the hypersphere (4) will be smaller so that whole momentum regions may collapse, or contribute in a much less pronounced way to the yield. For instance, for nonsequential quadruple ionization, for the absolute phase $\phi = 0$ the small peak on the positive momentum region is absent. This is due to the fact that the momentum space for the orbits $(5,6)$ is much smaller than in the three-electron case, so that their contributions to the yield are negligible. For $\phi = 0.8\pi$, we have also observed that the small peak in the negative momentum region is not present, for the same reason.

We now consider non-vanishing thermalization times and a constant absolute phase, which has been chosen so that the yield is almost entirely concentrated in the negative momentum region. The results of these computations

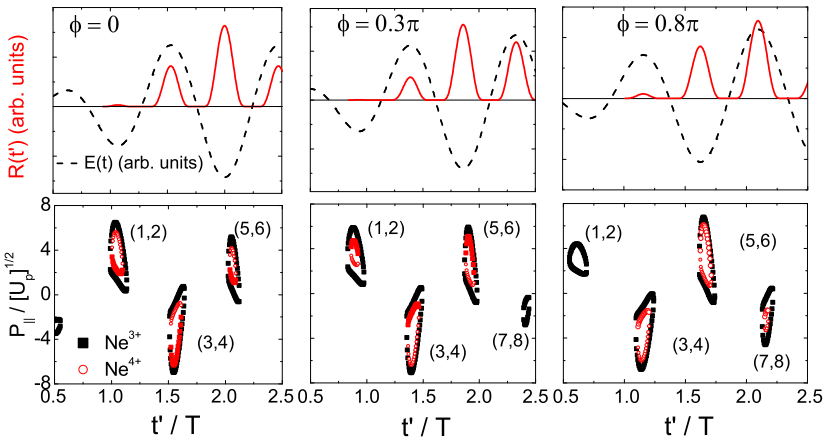

Figure 6. (Color online) Quasi-static tunneling rate (upper panels), and parallel momenta $P_{\parallel}$ (lower panels), as functions of the start times t', for triple and quadruple ionization of neon. We consider absolute phases $\phi = 0$, $\phi = 0.3\pi$ and $\phi = 0.8\pi$, the same driving-field parameters as in the previous figure, vanishing transverse momenta $P_{\perp}$ and thermalization times $\Delta t = 0$. The numbers (i, j) in the figure indicate a pair of orbits, with the odd and even numbers referring to the longer and the shorter orbit in a pair, respectively. The start time t' is given in units of the field cycle and the ion momenta in units of $[U_p]^{1/2}$.

are displayed in Fig. 7. As an overall feature, the time delays Δt influence the width and the position of the peaks of the distributions. They do not modify, however, their asymmetric shapes or the momentum region the yield is concentrated. This is due to the fact that a non-vanishing Δt changes the drift momenta the N electrons acquire from the external laser field when they reach the continuum, i.e., the left-hand side in Eqs. (4) and (5), but does not affect the quasi-static tunneling rate (1) or the binding energy the electrons must overcome [i.e., the right-hand side in Eqs. (4), (5)]. Therefore the dominant pairs of orbits remain the same. In other words, by changing Δt one influences the center of the hypersphere (4), but not its radius.

We shall now have a closer look at how the width of the distributions is affected by the interplay between the long and the short orbit. In Fig. 8, we display the ion momentum distributions for quadruple ionization in the few-cycle pulse case, together with the individual contributions from the long and the short orbits. For a few-cycle pulse, we define such orbits with respect to the pair which gives dominant contributions to the yield. For this specific parameter set, this means orbits $(3, 4)$ in Fig. 6. The long- and short-orbit contributions, i.e., the individual contributions from orbits 3 and 4, respectively, behave in a similar way to the monochromatic-field case (Figs. 1 and 3). Indeed, for vanishing thermalization times, the momentum distributions

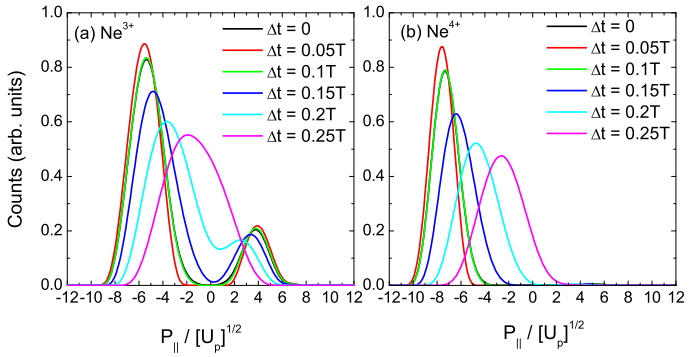

Figure 7. (Color online) Distribution of the longitudinal ion momentum for triple [panel (a)] and quadruple [panel (b)] nonsequential ionization of neon,for a four-cycle pulse of intensity at $I = 2 \times 10^{15}\mathrm{W/cm}^2$, absolute phase $\phi = 0$, and several time delays. The momenta are given in units of $[U_p]^{1/2}$.

from the slow-down collisions are peaked at a slightly larger absolute momentum than those from the short orbit. For $\Delta t = 0.1T$ [Fig. 8.(b)], the former and the latter contributions have moved away from or towards $P_{\|} = 0$, respectively. Once more, as the thermalization time increases, the peaks of both contributions shift towards vanishing ion momenta, as shown in Fig. 8.(c).

A qualitative difference, however, between Fig. 8 and its monochromatic counterpart is that, for large time delays, one no longer obtains a plateau in the vicinity of vanishing ion momenta, but a single peak in the negative momentum region. This is due to the fact that, for a monochromatic driving field, the symmetric peaks in the positive and negative momentum regions start to merge. For a few-cycle driving pulse, on the other hand, by taking an appropriate absolute phase, the distributions can be chosen in such a way that they are concentrated only in one momentum region. Hence, it is possible to avoid that a plateau or a single peak occurs near $P_{\|} = 0$.

4 Conclusions

We have investigated the influence of the shorter and the longer orbit of an electron recolliding inelastically with its parent ion on ion momentum distributions, within the context of a thermalization model for laser-induced $N-$fold nonsequential ionization. In this model, the first electron, upon recollision, shares the kinetic energy it acquired from the external laser field with the remaining $N-1$ bound electrons. All N electrons then leave after a time interval Δt. We have taken the driving field to be a monochromatic wave and a

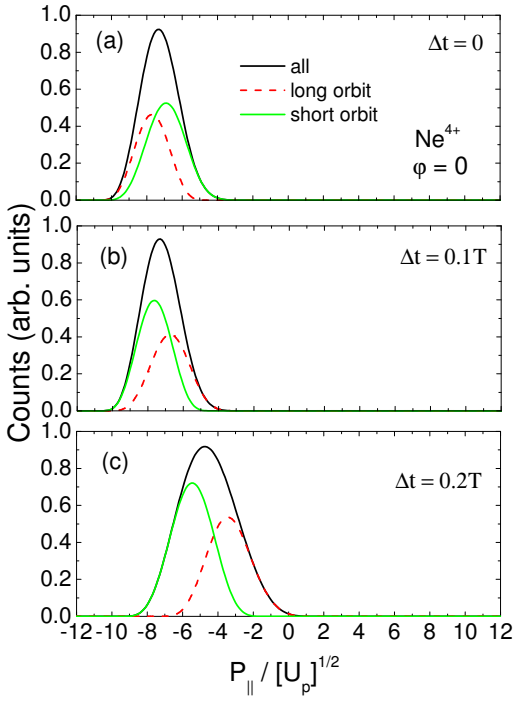

Figure 8. (Color online) Distribution of the longitudinal ion momentum quadruple nonsequential ionization of neon,together with the individual contributions from the long and short orbits, for a four-cycle pulse of intensity $I = 2 \times 10^{15}\mathrm{W/cm^2}$, absolute phase $\phi = 0$. We consider the time delays $\Delta t = 0$, $\Delta t = 0.1T$ and $\Delta t = 0.2T$. The ion momenta are given in units of $[U_p]^{1/2}$.

few-cycle laser pulse.

We have traced the variations in the widths and peaks of such momentum distributions, with respect to the time delays Δt, back to the momentum transfer from the field to an electron traveling along the short or the long orbit, and recolliding with its parent ion. The momentum transfer is maximal at a crossing of the electric field. With increasing time delays, the time for which the electrons released by a slow-down collision, i.e., by an electron moving along the long orbit, will leave their parent ion moves away from this crossing. As a direct consequence, the momentum transfer will decrease and the peak momenta will move towards lower absolute values. The situation is however quite different for the electrons released by a speed up collision. In this case, following the increase of time delay, the release time $t + \Delta t$ will initially (i.e., for $\Delta t \leq 0.05T$) approach a crossing, and subsequently (i.e., for $\Delta t > 0.05T$) move away from it. This will make the peaks of the pertinent momentum distributions move to larger absolute values, and then back towards $P_{\|} = 0$. The width of the resulting total momentum distributions, as well as their

peaks, will result from the interplay between such trends. This also explains the elongated patterns observed for the momentum distributions, in case the perpendicular momentum of the ion is resolved.

In both monochromatic and few-cycle cases, we considered the dominant pair of orbits, which, for each situation, is chosen in a slightly different way. For monochromatic fields, we took the two shortest trajectories, i.e., those for which the first electron spends the shortest time in the continuum. Physically, this pair is dominant, since the spreading of the electronic wave packet is less pronounced than for longer pairs of orbits. Hence, the overlap with bound-state wave packets will be appreciable[1]. In the few-cycle case, the dominant pair is determined by the interplay between the tunneling rate (1) for the first electron and the available momentum space. A pair of orbits will only contribute in a relevant way to the yield if the first electron is ejected with a large probability and if, upon return, it has enough energy to release the second electron (see, e.g. [9, 12], for more details).

Specifically for few-cycle pulses, we have shown that non-vanishing thermalization times do not play a very important role in determining the shape of the momentum distributions. This is due to the fact that a time delay $\Delta t \neq 0$ between recollision and multiple ionization only alters the drift momenta the N electrons acquire from the field when they reach the continuum. However, this delay does not modify the key ingredients which determine the dominant pairs of orbits and therefore the shape of the momentum distributions: the tunneling rate for the first electron and its kinetic energy upon return. In particular, both ingredients are highly dependent on the carrier-envelope phase, so that the shape of the momentum distributions can be used for measuring this parameter [12, 13]. This means that, even in case there is a non-vanishing thermalization time, one could, in principle, still employ nonsequential multiple ionization for absolute-phase diagnosis. Finally, few-cycle driving pulses may be very useful for testing and validating the thermalization model further, since many other ionization channels, such as excitation-tunneling or sequential ionization, are strongly suppressed in this case.

Acknowledgements: The authors would like to thank W. Becker for useful discussions. C.F.M.F. is also grateful to R. Moshammer and especially to A. Rudenko for discussions on nonsequential multiple ionization with few-cycle pulses, and to the Max Planck Institut für Kernphysik, Heidelberg, for its kind hospitality.

[1]We would like to stress out that wave-packet spreading is not included in our classical model. It is, however, present in the quantum-mechanical model we have employed in the two-electron case, which is its quantum-mechanical counterpart. In this latter case and as expected from our physical intuition, we verified that the main contributions to the yield come from the shortest pair.

References

[1] Th. Weber, M. Weckenbrock, A. Staudte, L. Spielberger, O. Jagutzki, V. Mergel, F. Afaneh, G. Urbasch, M. Vollmer, H. Giessen, and R. Dörner, Phys. Rev. Lett. **84**, 444 (2000).

[2] R. Moshammer, B. Feuerstein, W. Schmitt, A. Dorn, C.D. Schröter, J. Ullrich, H. Rottke, C. Trump, M. Wittmann, G. Korn, K. Hoffmann, and W. Sandner, Phys. Rev. Lett. **84**, 447 (2000).

[3] R. Dörner, Th. Weber, M. Weckenbrock, A. Staudte, M. Hattas, H. Schmidt-Böcking, R. Moshammer, and J. Ullrich, Adv. At. Mol. Opt. Phys. **48**, 1 (2002).

[4] M. Yu. Kuchiev, Pis'ma Zh. Éksp. Teor. Fiz. **45**, 319 (1987) [JETP Lett. **45**, 404 (1987)]; P. B. Corkum, Phys. Rev. Lett. **71**, 1994 (1993); K. C. Kulander, K. J. Schafer, and J. L. Krause, in *Proceedings of the SILAP Conference*, edited by B. Piraux et al (Plenum, New York, 1993), p. 95.

[5] A. Becker and F. H. M. Faisal, Phys. Rev. Lett. **84** 3546 (2000); ibid. **89**, 193003 (2002).

[6] R. Kopold, W. Becker, H. Rottke, and W. Sandner, Phys. Rev. Lett. **85**, 3781 (2000); S. V. Popruzhenko and S. P. Goreslavskii, J. Phys. B **34**, L239 (2001); S. P. Goreslavskii, S. V. Popruzhenko, R. Kopold and W. Becker, Phys. Rev. A **64**, 053402 (2001); S. V. Popruzhenko, Ph. A. Korneev, S. P. Goreslavskii and W. Becker, Phys. Rev. Lett. **89**, 023001 (2002); A. Heinrich, M. Lewenstein and A. Sanpera, J. Phys. B **37**, 2087 (2004).

[7] C. Figueira de Morisson Faria, X. Liu, W. Becker and H. Schomerus, Phys. Rev. A **69**, 012402(R)(2004).

[8] C. Figueira de Morisson Faria, H. Schomerus, X. Liu and W. Becker, Phys. Rev. A **69**, 043405 (2004).

[9] C. Figueira de Morisson Faria, X. Liu, A. Sanpera and M. Lewenstein, Phys. Rev. A **70**, 043406 (2004).

[10] C. Figueira de Morisson Faria, X. Liu and W. Becker, J. Mod. Opt. **53**, 193 (2006).

[11] E. Eremina, X. Liu, H. Rottke, W. Sandner, A. Dreischuh, F. Lindner, F. Grasbon, G. G. Paulus, H. Walther, R. Moshammer, B. Feuerstein and J. Ullrich, J.Phys. B **36**, 3269 (2003).

[12] X. Liu and C. Figueira de Morisson Faria, Phys. Rev. Lett. **92**, 133006 (2004).

[13] X. Liu, H. Rottke, E. Eremina, W. Sandner, E. Goulielmakis, K. O. Keeffe, M. Lezius, F. Krausz, F. Lindner, M. G. Schätzel, G. G. Paulus, and H. Walther, Phys. Rev. Lett. **93**, 263001 (2004).

[14] A. Rudenko, K. Zrost, B. Feuerstein, V. L. B. de Jesus, C. D. Schröter, R. Moshammer, and J. Ullrich, Phys. Rev. Lett. **93**, 253001 (2004).

[15] K. Zrost, A. Rudenko, Th. Ergler, B. Feuerstein, V. L. B. de Jesus, C. D. Schröter, R. Moshammer and J. Ullrich, J. Phys. B **39**, S371 (2006).

[16] X. Liu, C. Figueira de Morisson Faria, W. Becker and P. B. Corkum, physics/0506187 (J. Phys. B, in press).

[17] R. Hagedorn, Nuovo Cimento Suppl. **3**, 147 (1965).

[18] See, e.g., W. Forst, *Theory of Unimolecular Reactions* (Academic, New York, 1973); P.J. Robinson and K.A. Holbrook, *Unimolecular Reactions* (Wiley-Interscience, New York, 1972).

[19] B. Feuerstein, R. Moshammer, D. Fischer, A. Dorn, C.D. Schröter, J. Deipenwisch, J.R. Crespo Lopez-Urrutia, C. Höhr, P. Neumayer, J. Ullrich, H. Rottke, C. Trump, M. Wittmann, G. Korn, and W. Sandner, Phys. Rev. Lett. **87**, 043003 (2001).

[20] V. L. B. de Jesus, B. Feuerstein, K. Zrost, D. Fischer, A. Rudenko, F. Afaneh, C. D. Schröter, R. Moshammer, and J. Ullrich, J. Phys. B **37**, L161 (2004).

[21] See, e.g., P. Antoine, A. L'Huillier and M. Lewenstein, Phys. Rev. Lett. **77**, 1234 (1996); P. Salières, B. Carré, L. L. Déroff, G. G. Paulus, H. Walther, R. Kopold, W. Becker, D. B. Milošević, A. Sanpera, M. Lewenstein, Science **292**, 902 (2001); L. E. Chipperfield, P. L. Knight, J. W. G. Tisch and J. P. Marangos, Opt. Comm. (in press).

[22] R. Panfili, S. L. Haan and J. H. Eberly, Phys. Rev. Lett. **89**, 113001 (2002).

[23] C. Figueira de Morisson Faria and W. Becker, Laser Phys. **13**, 1196 (2003).

[24] T. Brabec and F. Krausz, Rev. Mod. Phys. **72**, 545 (2000); D. B. Milošević, G. G. Paulus, D. Bauer and W. Becker, J. Phys. B **39**, R203 (2006).

[25] L. D. Landau and E. M. Lifshitz, *Quantum Mechanics (Nonrelativistic Theory)* (Pergamon Press, Oxford, 1977).

[26] G. G. Paulus, W. Becker and H. Walther, Phys. Rev. A **52**, 4043 (1995); C. Figueira de Morisson Faria, M. Dörr, W. Becker and W. Sandner, Phys. Rev. A **60**, 1377 (1999).

[27] L. B. Fu, J. Liu, S. G. Chen, Phys. Rev. A **65**, 021406(R)(2002); J. Chen and C. H. Nam, Phys. Rev. A **66**, 053415 (2002).

[28] I. S. Gradsteyn and I. M. Ryzhik, *Table of Integrals, Series, and Products* (Academic Press, New York, 1980).